Journal of Sol-Gel Science and Technology (2023) 105:278–290
https://doi.org/10.1007/s10971-022-05965-z

ORIGINAL PAPER: SOL-GEL, HYBRIDS AND SOLUTION CHEMISTRIES

Effect of vanadium precursor on dip-coated vanadium oxide thin films

Mohammed Bouzbib[1] · János Rohonczy[2] · Katalin Sinkó[2]

Received: 7 September 2022 / Accepted: 11 October 2022 / Published online: 9 November 2022

Abstract

The effect of chemical substances is reported on the structure, surface morphology, and material properties of vanadium oxide thin films. The study of the chemical substances concentrated on the effects of initial materials (e.g., NH_4VO_3, $NaVO_3$, VO_2, vanadyl acetylacetonate, ammonium decavanadate) and various additives (e.g., acids, chelate ligand, reduction reagent, and tensides). The syntheses are based on sol-gel chemistry. The important aim of the sol-gel technique was to optimize the chemical conditions such as catalyst and solvent for the preparation of perfect V^{5+}-containing layers. The other aim was to check the controllability of the V^{4+}/V^{5+} ratios. The control was performed in the air by using a reducing agent and in a nitrogen atmosphere. The atomic and bond structures were investigated by ^{51}V MAS NMR, IR, and UV spectroscopies. The supramolecular structures were determined by SEM, EDX, and GIXRD techniques.

Graphical abstract

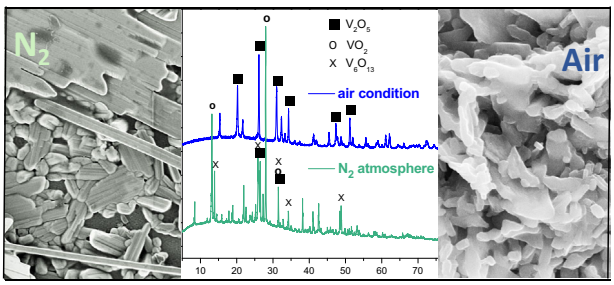

Keywords Vanadium oxide · Thin films · Dip coating · Optical and morphological properties

Highlights

- Complete, homogeneous, and transparent V^V-containing thin layers with orthorhombic structures from NH_4VO_3 and HNO_3.
- Complete and homogeneous V^{IV}-containing layers from VO_2 or vanadyl(IV) acetylacetonate in the presence or absence of reducing agents.
- Procedure of mixed oxidation states (V^{IV} and V^V) in air between 100 and 200 °C.

1 Introduction

In recent years, vanadium oxide thin film synthesis has attracted intensive interest due to its excellent properties such as good chemical and thermal stability [1], wide optical band gap, high electrical, and electrochromic properties [2]. These properties make vanadium oxides appropriate for various applications such as microelectronic, electrochemical,

✉ Katalin Sinkó
katalin.sinko@ttk.elte.hu

[1] Doctoral School of Environmental Sciences, Eötvös Loránd University, H-1117 Budapest, Hungary

[2] Institute of Chemistry, Eötvös Loránd University, H-1117 Budapest, Hungary

optoelectronic devices [3], gas sensing [4, 5], photoelectric devices [6], and optical switching devices [7].

Vanadium oxide systems possess different oxidation states from V^{2+} to V^{5+}. V_2O_5 is the most stable [1], but there are also VO, V_2O_3, and VO_2 as stable forms. Besides these systems, mixed-valence oxides also exit, e.g., Magnéli (V_nO_{2n-1}, $3 \le n \le 9$) and the Wadsley ($V_{2n}O_{5n-2}$) phases [8–10]. The coordination number in metal vanadate is 4 or 6. The semiconductivity of vanadium-containing systems depends on the valence state of vanadium. The electron transfer between lower and higher valence states (V^{4+} and V^{5+}) guarantees the n-type superconductivity. The orthorhombic crystallographic structure of vanadium pentoxide (V_2O_5) is the most stable texture of the vanadium oxides [1]. The V_2O_5 possesses a weak electric character in α, ε, δ, and γ crystalline phases. However, the amorphous $V_2O_5 \cdot H_2O$ shows much stronger electrical properties, e.g., high specific electrical capacity. The electrical conductivity of $V_2O_5 \cdot H_2O$ may be electronic and ionic owing to the water content. V^{3+}- V^{4+} and V^{4+} - V^{5+} mixed oxides (e.g., V_6O_{13} or V_4O_{10}) have also special electrical properties. Vanadium (IV) oxide thin films have attracted a lot of attention for many advanced applications such as battery materials [11], gas sensing, data storage [12], optical computing [13], and infrared modulators in missile guidance systems [14]. The reason for those advanced applications is due to the variety of potential phases of VO_2. Small crystal lattice discrepancies cause major measurable changes in the structural and electrical properties [13].

Vanadium pentoxide (V_2O_5) thin films can be prepared by various methods such as pulsed laser deposition [15], spray pyrolysis [16, 17], chemical vapor deposition [18, 19], sol-gel technique [20, 21], spin coating [22], atomic layer deposition [11], thermal evaporation [10], sputtering [23], and dip coating methods [24]. Dip coating is a low-cost and easy experimental setup for layer formation. The uniformity, quality, and reproducibility of the films can be controlled by several factors such as immersion time and dipping rate [25, 26]. Margoni et al. studied the effect of substrate temperature on the structural, optical, morphological, and electrical properties of V_2O_5 by adding nitric acid [27]. Chu et al. prepared nanostructure V_2O_5 film using oxalic acid in a hydrothermal treatment [28]. George et al. reported the preparation of V_2O_5 by dip coating using polyethylene glycol and nitric acid [29].

V(IV) oxide thin film can be synthesized by solution-based synthesis including various methods, sol-gel methods [30], polymer-assisted deposition [31], and hydrothermal synthesis [32] over the melt-quenched method. In contrast to gas-phase methods, solution-phase methods are more simplified and more cost-effective setup [33].

In the present work, the effect of preparation conditions is reported on the structure, surface morphology, and material properties of vanadium oxide thin films. To study the effect of starting materials, the cations of vanadate compounds (e.g., H^+, NH^{4+}, Na^+) or the additives on the structure and material properties is an emphasized task. The syntheses are based on sol-gel chemistry. The layered structure, morphology, and special material properties such as nanoporosity and functional behavior can be excellently regulated by the application of the sol-gel method. The ^{51}V MAS NMR spectroscopy is the leading structure investigation method. The important aim of NMR measurements was to correctly identify the vanadium ions with different oxidation states (V^{IV}, V^{V}) and to determine the ratio of different vanadium ions. The ratio of V^{IV} and V^{V} possesses a substantial role in the electric properties [34].

2 Experimental

2.1 Synthesis

Sol-gel synthesis was the fundamental preparation technique. Thermal decomposition was used as a complementary method and the melting process is provided for the comparison. Ammonium metavanadate (NH_4VO_3, Merck, ≥99% purity); volatile vanadate salts; our creation ammonium decavanadate ($(NH_4)_6[V_{10}O_{28}]$) as V^{5+}-containing precursor; and vanadyl acetylacetonate ($VO(acac)_2$, Merck, ≥99%); VO_2 (Merck, 98%) as V^{4+}-containing precursors were used in the syntheses. The effect of various chemical additives (acids, chelate ligand, reduction reagent, and tensides) was tested on the layer quality. Dip-coating techniques were used for the fabrication of vanadium oxide thin films on glass substrates at 400 °C.

2.1.1 Synthesis starting from NH_4VO_3

Ammonium metavanadate (NH_4VO_3) is dissolved in distilled water (0.21 mol dm^{-3}) and stirred at 50 °C. Without an acidic medium is not possible to obtain a clear solution, only yellow sols. To get a clear system, the pH of the medium must be 2, and H_3VO_4 forms in the orange solution. During the synthesis the acid reagents were varied, HNO_3, acetic acid (HAc), and citric acid were added. Besides acids, a cation exchange was applied to obtain H_3VO_4. In several experiments chemical additives (oxalic acid of 40 w/w % of metavanadate; ascorbic acid of 120 w/w % of metavanadate; ethyl acetate of 30–50 w/w % of metavanadate); and various surfactants (Pluronic L61, polyoxyethylene block copolymer), non-ionic Triton X 100 (glycol tert-octyl phenyl ether), cationic CTAB (cetyltrimethylammonium bromide) in 5–10 w/w % were also applied. These systems are suitable for dip-coating. The optimal concentration for dipping is 35 w/w % of metavanadate. The dip-coating is more effective and the layers have better quality in the presence of surfactants. The heat treatment is carried out at 70 and 400 °C (Fig. 1).

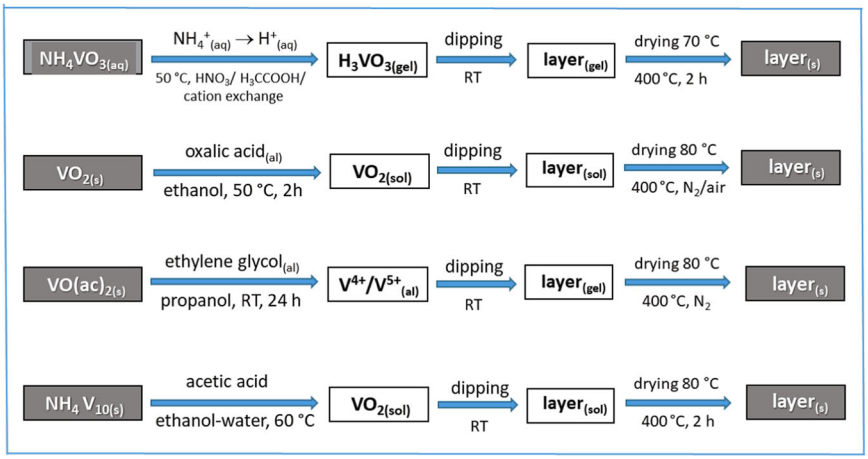

Fig. 1 Outline of various synthesis routes. $VO(ac)_2$: vanadyl(IV) acetylacetonate. NH_4V1_0: ammonium decavanadate

2.1.2 Synthesis starting from VO_2

VO_2 is dispersed in ethanol (20 g dm^{-3}) and oxalic acid (10 g dm^{-3}) is added. The solution is stirred at 50 °C for 2 h to get a sol solution. The substrate can be dipped in this sol solution to obtain layers. The layers are treated at 80 and 400 °C (Fig. 1).

2.1.3 Synthesis starting from vanadyl acetylacetonate, $VO(ac)_2$

Vanadyl acetylacetonate ($VO(C_5H_7O_2)_2$) is dissolved in propanol at a concentration of 0.125 mol dm^{-3}. The solution is stirred at room temperature for 24 h. Dipping of the layer can be realized from this vicious system. The viscosity of alcoholic solutions can be increased by ethylene glycol. The layer is dried at 80 °C for 1 h. The heat treatment must be carried out between 400 and 600 °C, N_2 atmosphere must be used to avoid the oxidation of V^{4+} to V^{5+} (Fig. 1).

2.1.4 Synthesis starting from ammonium decavanadate

The most stable form of V_{10} can be achieved in acidic conditions (pH 3–6). A decavanadate salt, $[V_{0.50}(H_2O)_5]_2[H_2(V_{10}O_{28})]\cdot 4(H_2O)$, was obtained by the reaction of $NaVO_3$ with quinhydrone (in 1:3 molar ratio) in a medium of pH 5–6 adjusted with glacial acetic acid. The mixture of reactants is dissolved in the ethanol-water mixture (40:60 v/v) and refluxed at 60 °C with stirring. After 1 day, the complex formation can be observed. But, instead of a vanadium-chinhydrone complex, a decavanadate salt, which does not contain chinhydrone, has been obtained. The solution of ammonium decavanadate can be directly applied for layer formation. The layers are treated at 80 and 400 °C (Fig. 1).

In dip-coating thin film preparation, the glass substrates were cleaned with acetone, ethanol, and deionized water by the ultrasonic bath. The substrates were dipped in the colloidal solution for 2 min with a withdrawing speed of 30 mm/min by an automated dip-coater (PTL-MM01 Dip Coater). The films were generally dried at room temperature in the air and heat-treated at 400 °C. This process was done between single and ten times.

2.2 Investigation methods

2.2.1 Scanning electron microscopy (SEM)

The surface covering and the layer thickness have been studied by an FEI Quanta 3D FEG scanning electron microscope. The SEM images were prepared by the Everhart-Thornley secondary electron detector (ETD), its ultimate resolution is 1–2 nm. Since the conductance of the particles investigated is high enough to remove the electric charge accumulated on the surface, the SEM images were performed in a high vacuum without any coverage on the specimen surface. For the best SEM visibility, the particles were deposited on a HOPG (graphite) substrate surface. SEM combined with energy disperse X-ray spectroscopy (EDX) is mainly applied for spatially resolved chemical analysis of monolith samples.

2.2.2 Reflection optical microscopy (ROM)

The surface of layers has also been investigated by reflection optical microscopy, which is part of the AFM instrument (Park System, XE-100, South Korea) Measurements were performed in air at 25 °C in non-contact mode.

Grazing incidence X-ray diffraction (GIXRD) measurements were performed by a Rigaku Smartlab X-ray diffractometer equipped with a 1.2 kW copper source (radiation wavelength: CuKα; $\lambda = 0.15418$ nm). To reduce the effect of the substrate, a grazing incidence parallel-beam geometry was used with an incidence angle of $\omega = 1°$. Scans were performed in the range 2Θ between 10° and 110° with a 1D silicon strip detector (D/Tex ultra-250) at a speed 0.2°/min.

2.2.3 UV-Visible spectroscopy

The transmittance of thin films was determined by UV-visible spectroscopy using Dynamica spectrophotometer with UV detective program) at room temperature, in the range of 200–1000 nm.

The IR spectra were recorded on a Bruker Alpha Fourier transform spectrometer equipped with a single reflection diamond ATR unit using a resolution of 2 cm^{-1}.

^{51}V (I = 7/2, 99,75% abundance) nuclear magnetic resonance spectroscopy (NMR) measurements were performed on Bruker Avance-III NMR spectrometer with a 4 mm MAS probe at 11.744 Tesla. All samples were measured at 131.48 MHz resonance frequency with a single pulse sequence using a 15-degree flip angle, and a 1 s relaxation delay. 2 K data points were accumulated at 9, 10, or 11 kHz MAS rotation speed. Typically 1024 FID signals were accumulated to increase the signal-to-noise ratio. 4 K real spectrum points were calculated applying zero filling and 100–500 Hz line broadening on the FID data points. $VOCl_3$ was used for the external standard of the ppm scale. Vanadium(V) spectra were observed in a 4750 ppm spectrum window. Vanadium(IV) nuclei were measured in a 9500 ppm wide window because of their bigger CSA, quadrupole, and paramagnetic anisotropy. The very wide spectrum range resulted in strong baseline distortions of the spectra which were eliminated by a modified SOLA computer simulation program of BRUKER TopSpin software. The advantageous possibility of ^{51}V NMR measurements are: vanadium isotope frequency of 99.75%, well measurable in oxidation state of 5+, the evaluation of ^{51}V NMR spectra is reliable and unambiguous however, raise a problem.

3 Result and discussions

3.1 Effect of vanadium precursors

3.1.1 NH_4VO_3 precursor

The starting vanadium-containing materials have strong effects on the layer structure.

Using NH_4VO_3 the most important step is to create pH ≈ 2 in the initial solution to get H_3VO_4 molecules. Only the molecules of H_3VO_4 are able for condensation reactions and to form a 3D network. The charges of VO_3^- the anion prevents the condensation leading to the formation of polyvanadates. In the experiments of NH_4VO_3, only vanadium(V)-containing materials have been prepared. The optimal concentration for dipping is 35 w/w % of metavanadate solution. The quality of the layers strongly depends on even the acidification beside the V-precursor (See in 3.2 section!).

3.1.2 Vanadyl(IV) acetylacetonate precursor

The aim of the application of vanadyl(IV) acetylacetonate ($VO(acac)_2$) was to prepare a V^{IV}-containing layer. V^{IV}-content is needed for more intensive electrical properties [34]. VO_2 was proved to have better electrochemical performance compared with V_2O_5 [35]. $VO(acac)_2$ has several advantages compared to vanadium alkoxides as typical sol-gel precursors. $VO(acac)_2$ can be characterized by its low price, low toxicity, highly stable against precipitation, and rapid hydrolysis. From $VO(acac)_2$ an ester forms by elimination of a C_3H_4 group, which transforms into anhydride in the first step, then into VO_2 by further heat treatment [36].

$$VO(acac)_2 + H_2O \rightarrow Hacac + acacVOOH \quad (1)$$

$$HacacVOOH + H_2O \rightarrow VO(OH)_2 \quad (2)$$

The synthesis and the heat treatment must be performed in a humid N_2 atmosphere to obtain VO_2 film. The precursor films can turn into crystalline VO_2 by the heat treatment [36]. The final heat treatment needs 500–600 °C for efficient (monoclinic or orthorhombic) crystallization of VO_2. The layer dipped from the viscous solution of $VO(acac)_2$ and dried in the air proved to be not homogeneous, NaCl phase separation of 1.5–2 µm particles can be observed by SEM and EDX techniques (Fig. 2, ×5000 magnification). The samples heat treated in air consist of

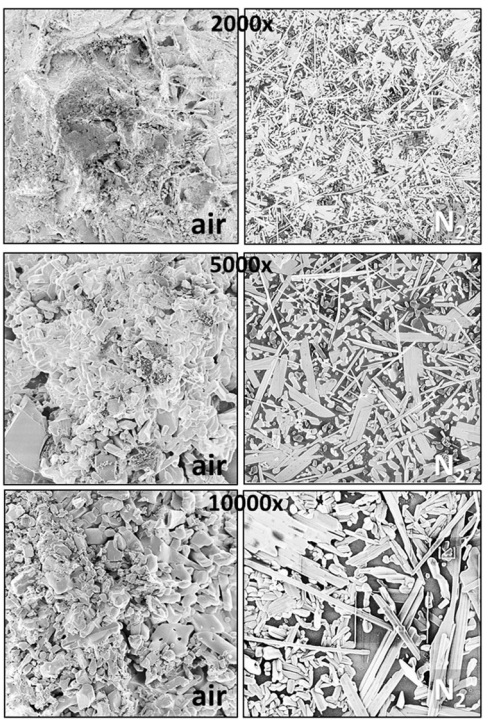

Fig. 2 SEM images. The samples were prepared from $VO(acac)_2$ and heated in air and N_2 atmosphere

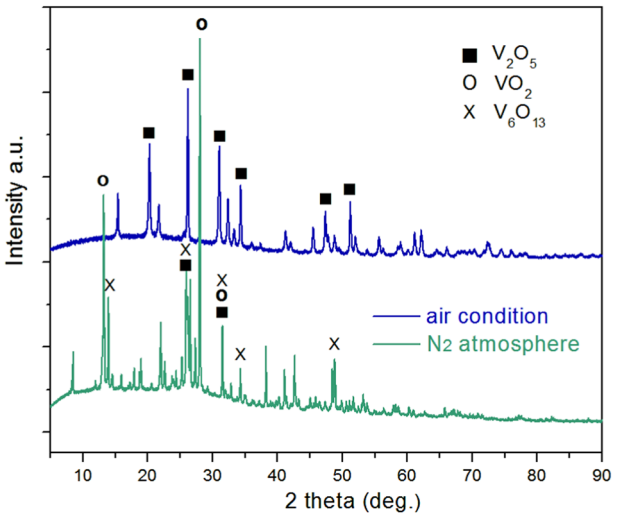

Fig. 3 XRD patterns. The vanadium oxide thin films were prepared from $VO(acac)_2$ and heated in air and N_2 atmosphere

anisotropic particles: 200–500 nm × 500–1000 nm (Fig. 2). The structure of samples heat treated in N_2 is composed of VO_2 nanorods/fibers (Fig. 2). The nanorods/fibers can be characterized by narrow size distribution: the average diameter is 135 nm ± 20 nm, the average length is 7.7 ± 2 µm.

The crystalline phases of the layers prepared from $VO(acac)_2$ and heated in a nitrogen atmosphere and for comparison in the air at 500 °C are represented in Fig. 3. The XRD data proves that the vanadate sample heated at 500 °C in the air can be characterized only by the V_2O_5 crystalline phase (26°, 110 planes). The identification was carried out using card #98-002-2114. The sample heated at 500 °C in N_2 possesses multiple crystalline structures (Fig. 3). The dominant phase is VO_2 (28°, 110 plane, and 13.3°, JCPDS card #65-7960) due to using an N_2 atmosphere during the heating. VO_2 coexists with the V_6O_{13} monoclinic crystalline phase appears at 13.97°, 26°, 26.5°, 34°, and 48.7° (JCPDS card #71-2235). V_6O_{13} has a mixed vanadium state of V^{4+} (four) and V^{5+} (two), the tunnel-like V_6O_{13} comprises alternative single and double vanadium oxide layers with shared corners. The presence of a small amount of a single V_2O_5 phase (26°, 31.4°) cannot be excluded. Both oxides (VO_2 and V_6O_{13}) can be well utilized as cathode materials.

The ^{51}V NMR measurements of systems synthesized from $VO(acac)_2$ could not be realized due to the strong disa dvantageous interactions derived from chemical shift anisotropy (CSA); paramagnetic electrons of V^{IV}; and quadrupole interaction with asymmetric electron environments. The paramagnetic electrons result in wide overlapping of rotation sidebands. Thus, the exact evaluation of NMR spectra was not possible, but the spectra do not confirm any presence of V^V neither in precursor materials nor in the final layer materials heated in N_2.

3.1.3 VO_2 precursor

The aim of experiments with VO_2 dispersed in ethanol and oxalic acid was to check the chemical and structural changes of VO_2 in the function of heating temperature. The oxalic acid may have a reduction effect even in the air [37]. The changes in chemical structure were investigated by ^{51}V NMR. The determination of vanadium oxidation number in solid materials is not a trivial task even by MAS NMR spectroscopy. The NMR signals of vanadium with various oxidation states may help appear very far from each other in the spectrum. The vanadium ion with 7/2 nuclear spin, 99.75% natural abundance and +5 oxidation state can be well detected by NMR in the solutions. In solid phases, the identification is more difficult. The spectrum range of near 4000 ppm, a quadrupole coupling of a few MHz, an anisotropic shading of 1000 ppm, a line broadening of 5000 Hz due to the quadrupole relaxation, strong baseline deformation, and many spinning sidebands make the evaluation of spectra more difficult.

The ^{51}V NMR results are summarized in Fig. 4. At the room temperature stable monoclinic β-VO_2 transforms into rutile α-VO_2 at 68 °C, which turns back into again β-VO_2 at room temperature. Thus, this phase transformation cannot be detected by NMR at room temperature.VO_2 starts to be oxidized in the air already at 200 °C (Fig. 4). V_2O_5 phase can be detected in the sample treated at 200 °C. The oxidation will be more intensive at 350 °C and completed at 500 °C. VO_2 phase disappears at this temperature. According to these NMR results, mixed oxidation states (V^{IV} and V^V) can be achieved by heating in the air only between 100 and 200 °C. The electrical properties of vanadate systems can be most effectively regulated by the vanadium's charge of structural units, the ratio of V^{IV} and V^V [34].

The surface of the layer prepared from VO_2 sol solution in the room temperature is not smooth (Fig. 5). It consists of some small and some larger particles due to the sol system. According to the EDX, every particle consists of vanadium and oxygen.

3.1.4 Ammonium decavanadate precursor

The orange ammonium decavanadate $(NH_4)_6[V_{10}O_{28}]$ that contains 10 vanadium atoms is a stable species for several days at neutral pH, but at higher pH immediately converts to the structurally and functionally distinct lower oxovanadates such as the monomer, dimer or tetramer. The most stable form of V10 is in the acidic pH range (pH 3–6). Decavanadate anions consist of three chemically different vanadium sites; the metal sites at the central junction correspond to two central VO_6 octahedra containing only bridging oxygen atoms, and two types of peripheral vanadium units including a V=O bond are assembled around the

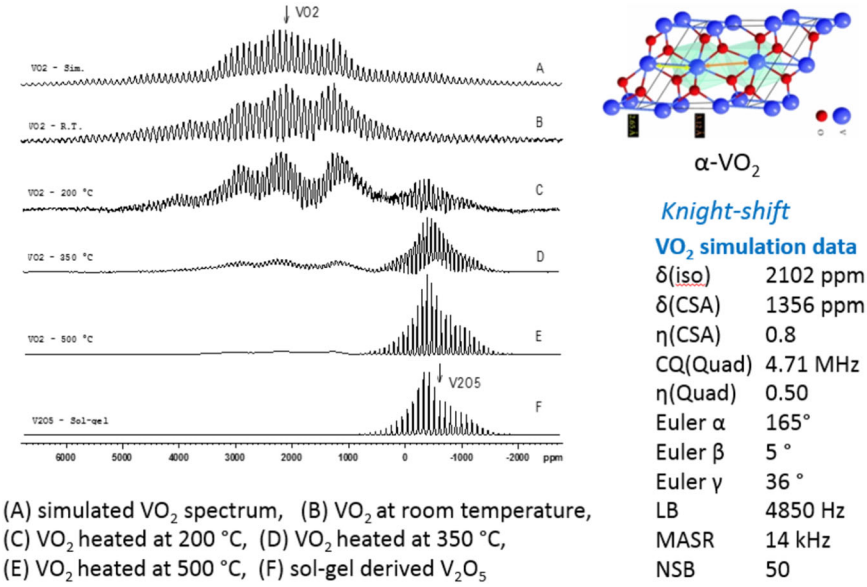

Fig. 4 ^{51}V NMR spectra of VO_2 vs. temperature. V_2O_5 provides for comparison

(A) simulated VO_2 spectrum, (B) VO_2 at room temperature, (C) VO_2 heated at 200 °C, (D) VO_2 heated at 350 °C, (E) VO_2 heated at 500 °C, (F) sol-gel derived V_2O_5

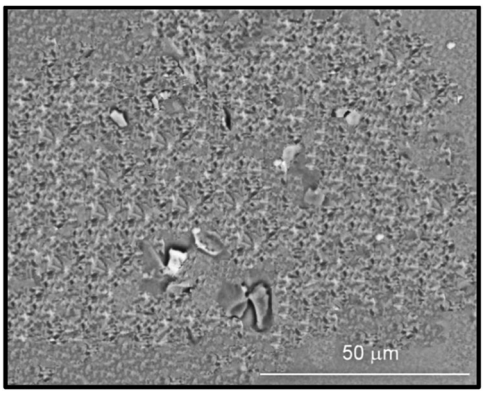

Fig. 5 SEM images of vanadate layers prepared from VO_2 sol solution

central units [38]. Although the solution of ammonium decavanadate covers excellently the surface of the glass substrate, the layer is destroyed after a drying process. Various rates, temperatures, and atmospheres of drying were checked out but without success. The material of the substrate was changed from glass to carbon, which results in layers with low quality already in the wet state.

The ^{51}V MAS NMR spectrum exhibits dozens of sidebands in the wide frequency range of 1800 ppm to −2800 ppm (Fig. 6). The strong CSA and quadrupole couplings were determined for these sites by computer simulation. Three kinds of decavanadate sites were identified at −418 ppm (δCSA = −1192 ppm, ηCSA = 0.92, $C_Q = -2.06$ MHz, $\eta_Q = 0.99$), −504 ppm (δCSA = −2151 ppm, ηCSA = 0.94, $C_Q = -3.99$ MHz, $\eta_Q = 0.6$) and −514 ppm (δCSA = −373 ppm, ηCSA = 0.44, $C_Q = -0.01$ MHz, $\eta_Q = 0.19$) according to the cluster structure of the anion [39]. The evaluation was carried out by a modified SOLA computer simulation program of BRUKER.

3.2 Effect of acidic catalysts and chemical additives

The effects of catalysts and other chemical additives are represented by means of samples prepared from the most promising precursor, $\mathbf{NH_4VO_3}$. Starting from NH_4VO_3, the compulsory step of synthesis is to create pH ≈ 2 in the initial solution. The pH value can be regulated by acids or cation exchanged.

- From the various acids used for setting pH ≈ 2, the application of HNO_3 results in complete and transparent layers (Fig. 7). Using nitric acid catalyst produces a 3D colloid network, which is built up of randomly connected compact particles of 0.6–0.8 µm size. The layer provides a continuous, porous, and transparent coating (Fig. 7).
- No homogeneous layers form using HCl or citric acid. The layer prepared with citric acid is not complete is set up from fibers, and filaments. Besides the filaments, there are some nano-sized fragments. The typical length of fibers is 4–5 µm (Fig. 7).
- Oxalic and ascorbic acids are too weak to get pH ≈ 2, but they may also have a weak reduction effect [40–42]. The reduction may lead to the formation of V^{IV} ions. But in these series, no measurable reduction could be detected by NMR, only V^V could be demonstrable. Acidification by proton exchange increases the coordination of V^V from 5 to 6. An exemplar for hexacoordinated species: $[VO(OH)_3(OH_2)_2]$. Using oxalic acid produces no homogeneous coating. The particles of 2–3 µm compose a compact layer on a limited surface. The other part of the substrate surface is covered with separated particles of 100–200 nm sizes (Fig. 7).
- The ascorbic acid does also not initiate a form of continuous and homogeneous layers or reduction of V^v

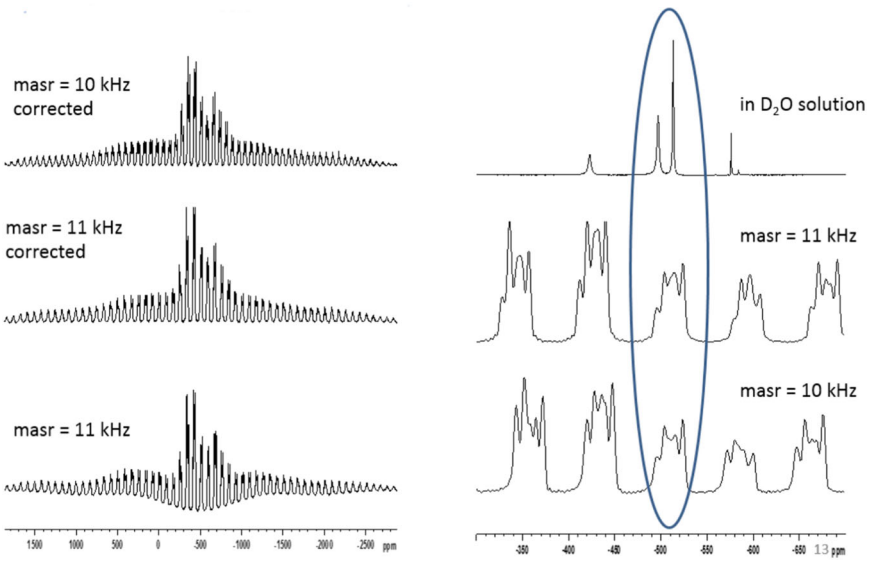

Fig. 6 ^{51}V NMR spectra of $(NH_4)_6[V_{10}O_{28}]$

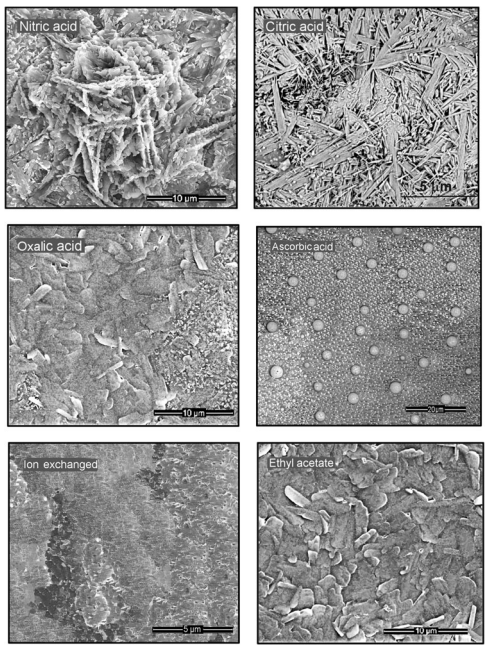

Fig. 7 SEM images of vanadate layers. The layers were prepared from NH_4VO_3 with various additives: nitric acid, citric acid, oxalic acid, ascorbic acid, ethyl acetate, and after ion exchange

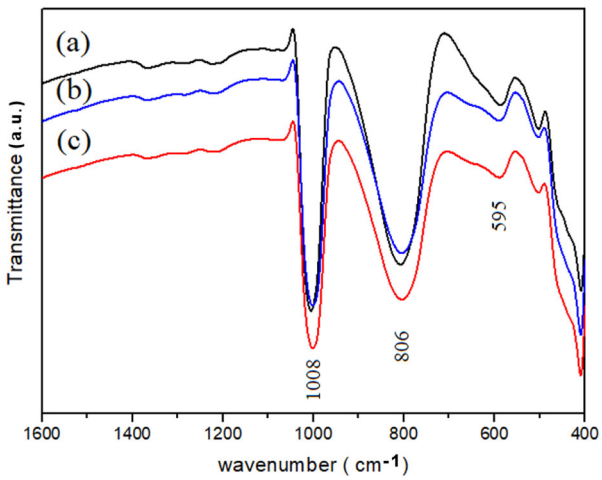

Fig. 8 FTIR spectra of vanadium pentoxide thin films. The films were prepared on glass substrates with different chemical additives: (**a**) ethyl acetate; (**b**) nitric acid; (**c**) oxalic acid

units. According to EDAX measurements, both types of particles represented in SEM image possess powerful V-content without any carbon content. Thus, the spherical larger particles (5 µm) may be amorphous V-containing particles and the smaller units (1–10 nm) crystalline (Fig. 7).

– The layer derived from an ion-exchanged solution is not continuous. The layer structure is built up from units of 100–300 nm and their aggregates of 4–6 µm (Fig. 7).
– The application of ethyl acetate also supports the formation of a compact, continuous covering. The main part of the particles are rods with ~500 nm diameter and ~3 µm length similar to the rods of systems produced from $VO(acac)_2$. Some plate-like particles (2–3 µm ∅) can also be observed. The particles are typified by narrow distribution (Fig. 7).

3.2.1 FTIR spectroscopy

FTIR was used to analyze the phase composition of vanadium oxide thin films (Fig. 8). Oxides possess distinct features below the frequency of 1200 cm^{-1}, at ~1008, 806, and 595 cm^{-1}. Three major vibration modes of the

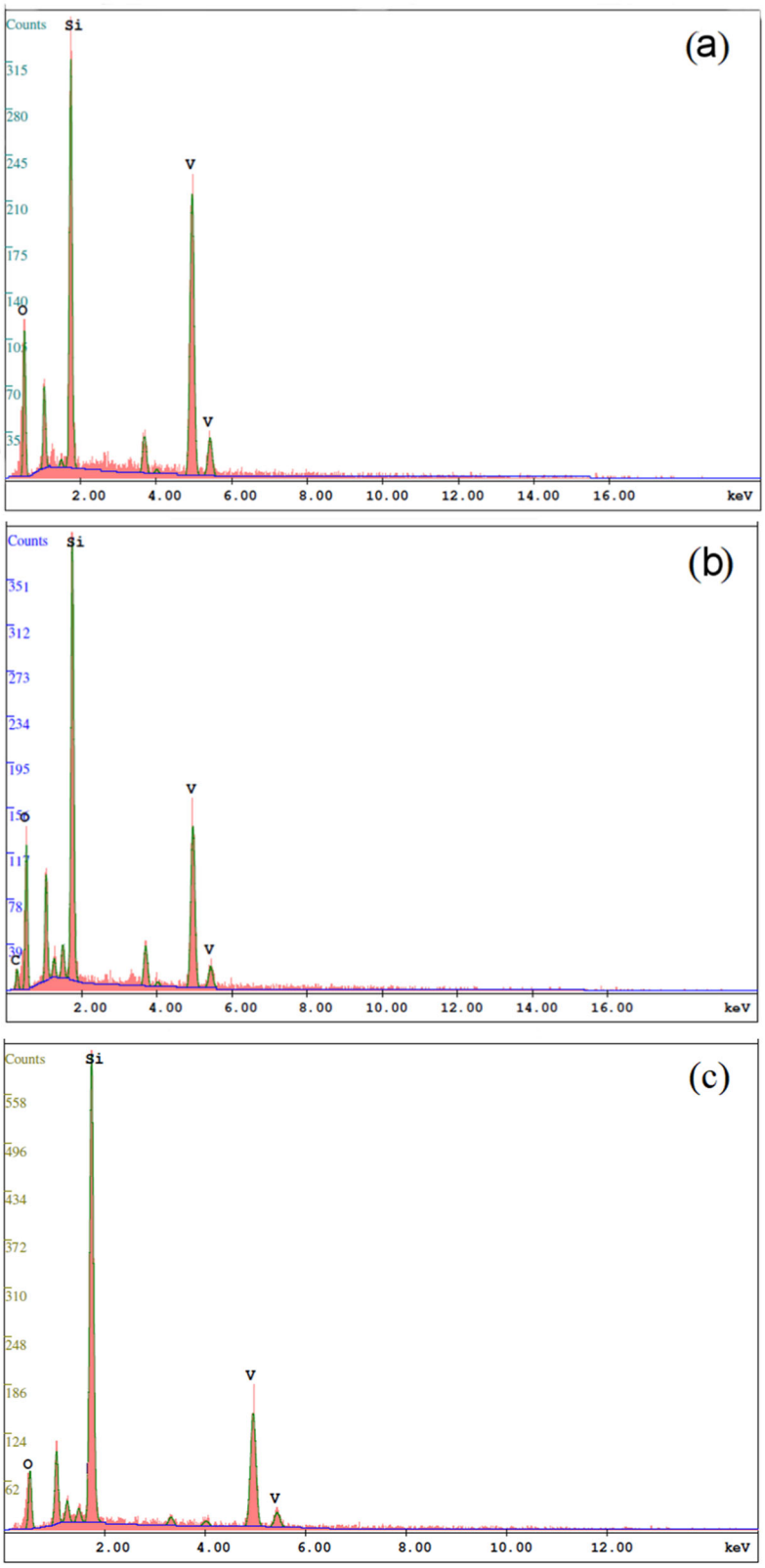

Fig. 9 Energy Dispersive X-ray Analysis (EDX) of vanadium pentoxide thin films, The films were prepared on glass substrates with different chemical additives: (**a**) nitric acid; (**b**) ethyl acetate; (**c**) oxalic acid

vanadium oxide correspond to the V=O symmetric stretching vibration; V-O–V asymmetric stretch, and the symmetric stretch of V-O–V, respectively. The intensity and the frequency of the V–O vibrational bands vary slightly in the range of 400–1012 cm^{-1} by the influence of different additives.

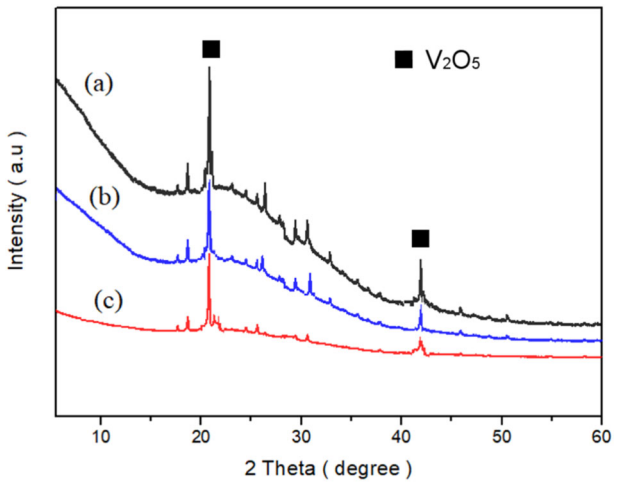

Fig. 10 XRD patterns of vanadium oxide thin films. The films were prepared on glass substrates with three types of most promising chemical additives: (**a**) nitric acid; (**b**) ethyl acetate; (**c**) oxalic acid

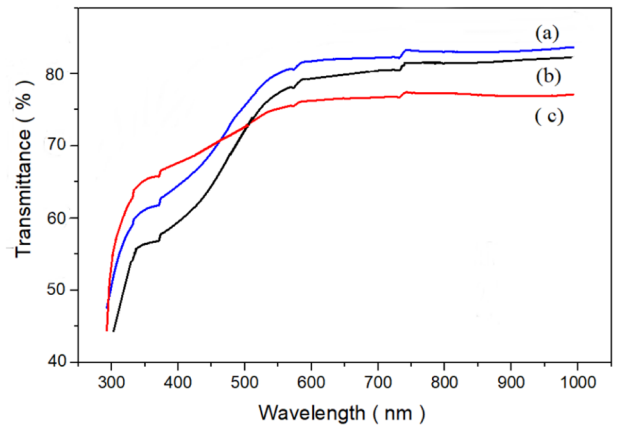

Fig. 11 Transmittance spectra of vanadium pentoxide thin films. The films were prepared on glass substrates with different additives: (**a**) nitric acid; (**b**) ethyl acetate; (**c**) oxalic acid

3.2.2 Energy dispersive X-ray analysis (EDX)

EDX technique provides information about the chemical composition of the thin layers (Fig. 9). The EDX spectra reveal the presence of vanadium (V) and oxygen (O) in the thin films. However, the presence of substrate peak (Si) is also prominent as the thickness of the film is so thin [43]. EDX also confirms the complete covering of film catalyzed by nitric acid (Fig. 9/a). This layer has the strongest vanadium content indicating more compact vanadium oxide cover. If its reason would be the major thickness of the layer thus, the oxygen content should be also larger.

3.2.3 X-ray powder diffraction (XRD)

The XRD measurements represent the crystallinity of the deposited vanadium pentoxide prepared with three types of most promising chemical additives (Fig. 10). The crystallization of the films occurs after annealing at 400 °C for 30 min in a muffle furnace. The use of various chemical additives (nitric acid, ethyl acetate, oxalic acid) does not produce detectable changes in crystallinity. The (101) peak intensity decreases with changing additive: (a) nitric acid; (b) ethyl acetate; (c) oxalic acid, respectively. The use of nitric acid results in the highest crystallinity in the films. The whole thin films show peaks (001) and (002) at 20.30° and 41.24° (2θ) respectively which confirm the presence of the V_2O_5 phase which corresponds to the orthorhombic system JCPDS file (JCPDS card #41-1426). The XRD measurements do not detect any V^{IV} content in the sample synthesized with oxalic acid.

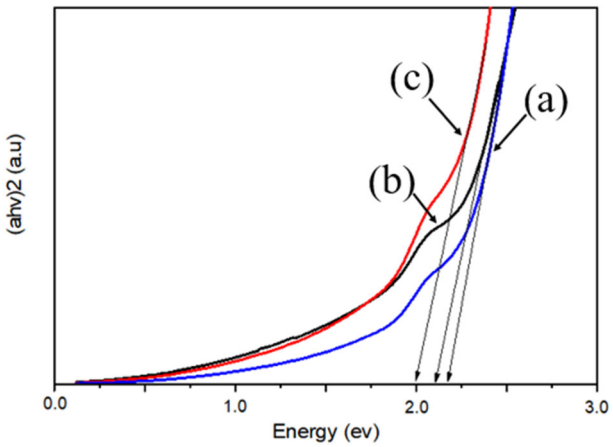

Fig. 12 The optical band gap (Eg) of vanadium oxide thin films: (**a**) ethyl acetate; (**b**) nitric acid; (**c**) oxalic acid

3.2.4 Optical behaviors

The transmittance spectrum of the vanadium pentoxide thin films prepared with various additives in the wavelength range from 250 to 1000 nm is shown in Fig. 11. In the wavelength range of 550–1000 nm, the film's transmittance of the films is >70%. The high transmittance indicates good homogeneity for thin film. The transmittance of the films decreased from nitric acid (a); to ethyl acetate (b) and oxalic acid (c), respectively. Maximum values of transmittance for the film are: nitric acid 81.2%; ethyl acetate 78.9%; and oxalic acid 74.4%.

The optical band gap (Eg) of vanadium oxide thin films prepared with different additives were calculated employing the Tauc plot: $(\alpha h\upsilon)^2 = A(h\upsilon - Eg)$. Where is α absorption coefficient, A is a constant, h is the Plank constant and Eg is the optical band gap (Fig. 12). The bandgap Eg can be estimated by extrapolation from the linear portion of the curves till they intercept the photon energy axis. The bandgap value calculated is 1.98 eV, 2.11 eV, 2.17 eV for the thin films prepared from oxalic acid, nitric acid, and

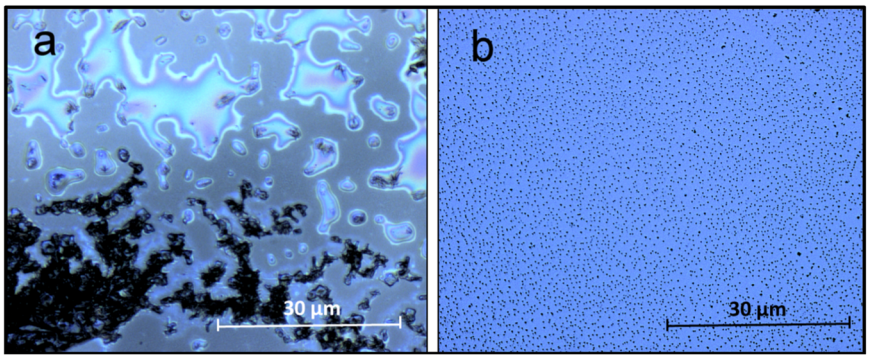

Fig. 13 Reflection optical microscopy images of vanadate layers prepared from NH_4VO_3 and nitric acid. The symbols: ***(a)*** without, ***(b)*** with surfactant (Triton X 100)

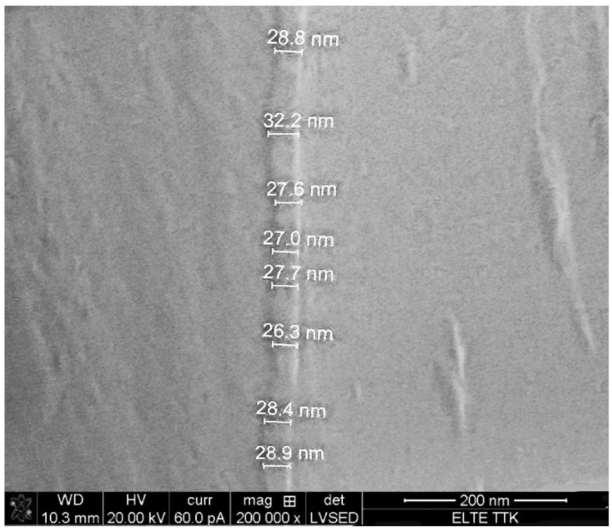

Fig. 14 SEM images of vanadium pentoxide thin films on glass substrates prepared with nitric acid

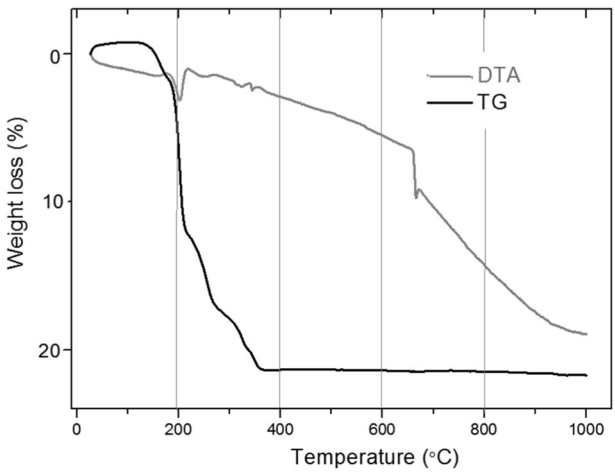

Fig. 15 TG curve of dried V-containing layer

ethyl acetate, respectively. It is important to note that the degree of non-stoichiometry and the thickness of the thin films are responsible for the variation in band-gap energy [29, 43–45].

3.3 Effect of tenside

The dip-coating is more effective and the layers have better quality in the presence of surfactants (Fig. 13). Triton X 100 proved to be the most effective of the various surfactants (Pluronic L61, non-ionic Triton X 100, cationic CTAB).

3.4 Characterization of vanadium oxide layers

Based on previous experiments, the most promising synthesis route for the V_2O_5 layer uses NH_4VO_3, nitric acid as catalyst, and Triton X 100 as tenside. The application of ethyl acetate also results in prosperous quality for the layers. The synthesis must be carried out at 70 °C for 5 h. From this aqueous viscous solution, a homogeneous thin layer can be drawn, the layer thickness is 26–32 nm by a single dipping (Fig. 14). According to the thermal analysis (TG) the mass of the layer changes until 360 °C (Fig. 15). Thus, the development of V_2O_5 crystallites requires 360–400 °C in this procedure. DTA indicates the escape of ammonia at 200 °C.

Based on ^{51}V MAS NMR measurements the vanadate ions turn into first the mixture of VO_2^+ and $V_3O_{10}^{5+}$ at 100 °C then into V_2O_5 (α-V_2O_5) at 300 °C (Fig. 16, Table 1). The V_2O_5 samples are thermally stable until the measured temperature of 600 °C (α-V_2O_5 and β-V_2O_5) (Fig. 16, Table 1).

4 Conclusion

One of the aims of this study was to optimize the chemical conditions for the preparation of V^V-containing layers derived from the sol-gel technique. NH_4VO_3, $NaVO_3$, and ammonium decavanadate $(NH_4)_6[V_{10}O_{28}]$ were tested as V-precursor, and HNO_3, HCl, citric acid, oxalic acid, and ascorbic acids as a catalyst to create the required pH ≈ 2. The use of NH_4VO_3 and HNO_3 results in the best, complete and transparent layers. XRD results indicate that the thin films have orthorhombic structures with a preferred

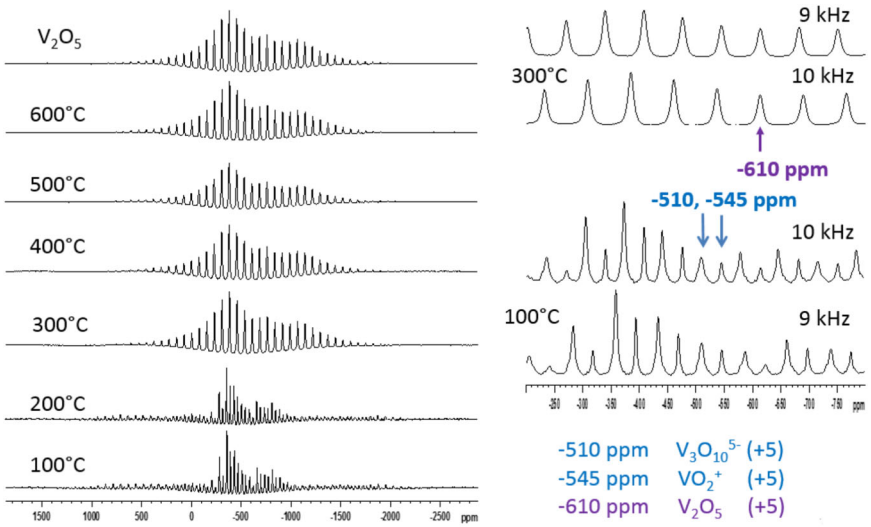

Fig. 16 ^{51}V NMR spectra of layer vs.temperature. The layer was synthesized from NH_4VO_3 and catalyzed with HNO_3 e

Table 1 ^{51}V NMR results

Sample	−508 – −509 ppm	−545 – −546 ppm	−610 ppm
NH_4VO_3, HNO_3, 100 °C	$V_3O_{10}^{5-}$ (+5)	VO_2^+ (+5)	
NH_4VO_3, HNO_3, 200 °C	$V_3O_{10}^{5-}$ (+5)	VO_2^+ (+5)	
NH_4VO_3, HNO_3, 300 °C			V_2O_5
NH_4VO_3, HNO_3, 400 °C			V_2O_5
NH_4VO_3, HNO_3, 500 °C			V_2O_5
NH_4VO_3, HNO_3, 600 °C			V_2O_5
V_2O_5 (RT)			V_2O_5
V_2O_5 heated at 500 °C			V_2O_5

orientation along (101) direction. The surface morphology appears to have changed due to the addition of different chemical substances. The UV-Visible spectroscopy analysis revealed that the average visible transmittance is all impacted by variation of chemical conditions. For thin films produced from oxalic acid, nitric acid, and ethyl acetate, the measured band gap values are 1.98 eV, 2.11 eV, and 2.17 eV, respectively.

Layers of good quality can be produced from ammonium decavanadate, but the layer is destroyed by a drying process. No homogeneous layers form using HCl or citric acid. Oxalic and ascorbic acids are too weak to get pH ≈ 2.

The other aim was to adjust various V^{IV}/V^{V} ratios. The ratio of V^{IV} and V^{V} possesses a substantial role in the electric properties. The complete and homogeneous layers can be prepared from VO_2 and vanadyl(IV) acetylacetonate in the presence or absence of reducing agents. Mixed oxidation states (V^{IV} and V^{V}) can be achieved in the air only between 100 and 200 °C according to NMR results. The oxalic and ascorbic acids suggested in the literature as reducing agents cannot prevent the oxidation to V_2O_5. The presence of V^{IV} can be held only in nitrogen atmosphere above 200 °C.

Author contributions All authors listed have made a significant contribution to the research reported and have read and approved the submitted paper, and furthermore, all those who made substantive contributions to this work have been included in the author list.

Funding Open access funding provided by Eötvös Loránd University.

Compliance with ethical standards

Conflict of interest The authors declare no competing interests.

Consent to publish All necessary permissions for publication were secured prior to submission of the paper.

Publisher's note Springer Nature remains neutral with regard to jurisdictional claims in published maps and institutional affiliations.

References

1. Margoni MM, Mathuri S, Ramamurthi K, Babu RR, Sethuraman K (2016) Investigation on the pure and fluorine doped vanadium

oxide thin films deposited by spray pyrolysis method. Thin Solid Films 606:51–56
2. Mjejri I, Rougier A, Gaudon M (2017) Low-Cost and Facile Synthesis of the Vanadium Oxides V_2O_3, VO_2, and V_2O_5 and Their Magnetic. Thermochromic and Electrochromic Properties. Inorg Chem 56:1734–1741
3. Abyazisani M, Bagheri-Mohagheghi MM, Benam MR (2016) Study of structural and optical properties of nanostructured V_2O_5 thin films doped with fluorine. Mater Sci Semicond Proc 31:693–699
4. Zakharova GS, Liu J, Enyashin AN, Yang X, Zhou J, Jin W, Chen W (2018) Metal cations doped vanadium oxide nanotubes: Synthesis, electronic structure, and gas sensing properties. Sens Actuators, B Chem 256:1021–1029
5. Grayli SV, Leach GW, Bahreyni B (2018) Sol-gel deposition and characterization of vanadium pentoxide thin films with high TCR. Sensors Actuators. A Phys 279:630–637
6. Kim HS, Chauhan KR, Kim J, Choi EH (2017) Flexible vanadium oxide film for broadband transparent photodetector. Appl Phys Lett 110:12–10
7. Park J, Ahn K, Yu S, An J, Lee TH, Kim MG (2018) Oxidation state control of solution-processed vanadium oxide thin-films and resistive switching of VO_2 thin-film in a metastable state. Thin Solid Film 648:69–75
8. Bahlawane N, Lenoble D (2014) Vanadium oxide compounds: Structure, properties, and growth from the gas phase. Chem Vap Depos 20:299–311
9. Zhu M, Zhang D, Jiang S, Liu S, Qi H, Yang Y (2021) Phase evolution and thermochromism of vanadium oxide thin films grown at low substrate temperatures during magnetron sputtering. Ceram Int 47:15491–15499
10. Beke S (2011) A review of the growth of V_2O_5 films from 1885 to 2010. Thin Solid Films 519:1761–1771
11. Mattelaer F, Geryl K, Rampelberg G, Dobbelaere T, Dendooven J, Detavernier C (2016) Atomic layer deposition of vanadium oxides for thin-film lithium-ion battery applications. RSC Adv 6:114658–114665
12. Sanger A, Kumar A, Jaiswal J, Chandra R (2016) A fast response/recovery of hydrophobic Pd/V_2O_5 thin films for hydrogen gas sensing. Sensors Actuators. B Chem 236:16–26
13. Manning TD, Parkin IP, Blackman C, Qureshi U (2005) APCVD of thermochromic vanadium dioxide thin films-solid solutions $V_{2-x}M_xO_2$ (M = Mo, Nb) or composites VO_2: SnO_2. J Mater Chem 15:4560–4566
14. Manning TD, Parkin IP (2004) Vanadium(IV) oxide thin films on glass and silicon from the atmospheric pressure chemical vapour deposition reaction of $VOCl_3$ and water. Polyhedron 23:3087–3095
15. Koussi EK, Bourquard F, Tite T, Jamon D, Garrelie F, Jourlin Y (2020) Synthesis of vanadium oxides by pulsed laser deposition and rapid thermal annealing. Appl Surf Sci 521:146–267
16. Darroudi N, Eshghi H (2020) Effects of nozzle-to-substrate distance and annealing atmospheres on V_2O_5 thin films prepared by spray pyrolysis technique. Mater Sci Eng B Solid-State Mater Adv Technol 262:114–726
17. Gavalas S, Gagaoudakis E, Katerinopoulou D, Petromichelaki V, Wight S, Wotring G, Aperathitis E, Binas V (2019) Vanadium oxide nanostructured thin films prepared by Aerosol Spray Pyrolysis for gas sensing and thermochromic applications. Mater Sci Semicond Proc 89:116–120
18. Drosos C, Jia C, Mathew S, Palgrave RG, Moss B, Kafizas A, Vernardou D (2018) Aerosol-assisted chemical vapor deposition of V_2O_5 cathodes with high rate capabilities for magnesium-ion batteries. J Power Sources 384:355–359
19. Rajeswaran B, Umarji AM (2020) Defect engineering of VO_2 thin films synthesized by Chemical Vapor Deposition. Mater Chem Phys 245:122230
20. Amala AC, Vignesh R, Geetha GV, Sivakumar R (2021) Electrochromic behavior of vanadium pentoxide thin films prepared by a sol–gel spin coating. Process Phys Status Solidi Appl Mater Sci 218:1–12
21. Li Y, Liu J, Wang D, Pan G, Dang Y (2018) Effects of the annealing process on the structure and valence state of vanadium oxide thin films. Mater Res Bull 100:220–225
22. Mukherjee D, Dey A, Esther AC, Sridhara N, Kumar DR, Rajendra A, Sharma AK, Kumar A (2018) Reversible and repeatable phase transition at a negative temperature regime for doped and co-doped spin coated mixed valence vanadium oxide thin films. RSC Adv 8:30966–30977
23. Rakshit A, Mukherjee M, Chakraborty S (2018) Effect of oxygen content on the electrical properties of sputter deposited vanadium oxide thin-films. Mater Sci Semicond Proc 88:127–131
24. Jin A, Chen W, Zhu Q, Yang Y, Volkov VL, Zakharova GS (2009) Structural and electrochromic properties of molybdenum doped vanadium pentoxide thin films by sol-gel and hydrothermal synthesis. Thin Solid Films 517:2023–2028
25. Ingole RS, Fugare BY, Lokhande BJ (2016) Influence of concentration and volume of precursor on the electrochemical properties of vanadium oxide thin films prepared by spray pyrolysis. AIP Conf Proc 1724:1–8
26. Salles P, Pinto D, Hantanasirisakul K, Maleski K, Shuck CE, Gogotsi Y (2019) Electrochromic Effect in Titanium Carbide MXene Thin Films Produced by Dip-Coating. Adv Funct Mater 29:1–9
27. Margoni MM, Mathuri S, Ramamurthi K, Babu RR, Sethuraman K (2017) Sprayed vanadium pentoxide thin films: Influence of substrate temperature and role of HNO_3 on the structural, optical, morphological and electrical properties. Appl Surf Sci 418:280–290
28. Chu J, Kong Z, Lu D, Zhang W, Wang X, Yu Y, Li S, Wang X, Xiong S, Ma J (2016) Hydrothermal synthesis of vanadium oxide nanorods and their electrochromic performance. Mater Lett 166:179–182
29. George A, Raj AD, Irudayaraj AA, Ray DMA, Venci X, Jayakumar G, Arumgam J, Kumar MS, Sundaram SJ, Kaviyarasu K (2019) Two step synthesis of vanadium pentoxide thin films for optoelectronic applications. Mater Today Proc 36:464–467
30. Chae BG, Kim HT, Yun SJ, Kim BJ, Lee YW, Youn DH, Kang KY (2006) Highly oriented VO_2 thin films prepared by sol-gel deposition. Electrochem Solid-State Lett 9:1–12
31. Du J, Gao Y, Luo H, Kang L, Zhang Z, Chen Z, Cao C (2011) Significant changes in phase-transition hysteresis for Ti-doped VO_2 films prepared by polymer-assisted deposition. Sol Energy Mater Sol Cells 95:469–475
32. Gao C, Xie X, He R, Yu B, Wu B, Luo Z, Liu P, Chen K, Xie W (2018) Hydrothermal synthesis of high quality free-standing VO_2 (B) thin film and its thermal resistance characteristics. Mater Lett 225:29–32
33. Devthade V, Lee S (2020) Synthesis of vanadium dioxide thin films and nanostructures.". J Appl Phys 128:231–101
34. Wu C, Feng F, Xie Y (2013) Design of vanadium oxide structures with controllable electrical properties for energy applications. Chem Soc Rev 42:5157–5183
35. Shi Y, Chou SL, Wang JZ, Li HZ, Liu HK, Wu YP (2013) In-situ hydrothermal synthesis of graphene woven VO_2 nanoribbons with improved cycling performance. J Power Sources 244:684–689
36. Nenashev RN, Mordvinova NE, Zlomanov VP, Kuznetsov VL (2015) Thermal decomposition of vanadyl acetylacetonate. Inorg Mater 51:891–896
37. Costa C (2018) Application of vanadium oxide nanoparticles in smart surfaces. Master Thesis, Universidade Nova de Lisboa.
38. Salt ND (2017) Synthesis, characterization and crystal structure of a novel decavanadate. J Chil Chem Soc 62:3610–3614
39. Evans HT (1966) The Molecular Structure of the Isopoly Complex Ion, Decavanadate ($V_{10}O_{28}^{6-}$). Inorg Chem 5:967–977

40. Livage J, Henry M, Sanchez C (1988) Sol-gel chemistry of transition metal oxides. Prog Solid State Chem 18:259–341
41. Liu M, Su B, Tang Y, Jiang X, Yu A (2017) Recent advances in nanostructured vanadium oxides and composites for energy conversion. Adv Energy Mater 7:1–34
42. Zhao L, Miao L, Tanemura S, Zhou J, Chen L, Xiao X, Xu G (2013) A low cost preparation of VO_2 thin films with improved thermochromic properties from a solution-based process. Thin Solid Films 543:157–161
43. Porwal D, Esther AC, Raddy IN, Sridhara N, Yaday NP, Rangappa D, Bera P, Anandan C, Sharma AK, Dey A (2015) Study of the structural, thermal, optical, electrical and nanomechanical properties of sputtered vanadium oxide smart thin films. RSC Adv 5:35737–35745
44. Liu F, Lai Y, Liu J, Wang B, Kuang S, Zhang Z, Li J, Liu Y (2010) Characterization of chemical bath deposited CdS thin films at different deposition temperature. J Alloy Compd 493:305–308
45. Asiabar MA, Mohaghegh Z, Ghodsi FE (2018) Synthesis and characterization of nanocrystalline vanadium oxide thin films: electrochemical behavior by annealing in different atmosphere. Appl Phys A Mater Sci Proc 124:51–60